

Ozone Cracking and Flex Cracking of Crosslinked Polymer Blend Compounds

M. F. Tse

ExxonMobil Chemical Company, Baytown, Texas 77520

Received 6 February 2006; accepted 8 June 2006

DOI 10.1002/app.25139

Published online in Wiley InterScience (www.interscience.wiley.com).

ABSTRACT: Ozone cracking and flex cracking of crosslinked elastomer blends of brominated isobutylene/*para*-methylstyrene copolymer (BIMSM) and unsaturated elastomers, such as polybutadiene rubber (BR) and natural rubber (NR), are studied. This saturated BIMSM elastomer, which is a terpolymer of isobutylene, *para*-bromomethylstyrene, and *para*-methylstyrene, functions as the ozone-inert phase of the blend. Ozone cracking is measured by the failure time of a tapered specimen under a fixed load in a high severity ozone oven, whereas flex cracking is ranked by the De Mattia cut growth.

The ozone resistance of BIMSM/BR/NR blends is compared to that of a BR/NR blend (with or without antiozonant) at constant strain energy densities. The effects of the BIMSM content in the blend, the structural variations of BIMSM, and the network chain length between crosslinks on these two failure properties, which are important in crosslinked compounds for applications in tire sidewalls, are discussed. © 2006 Wiley Periodicals, Inc. *J Appl Polym Sci* 103: 2183–2196, 2007

Key words: blends; elastomers; fillers; morphology; rubber

INTRODUCTION

Prolonged exposure of unstretched natural rubber (NR) to ozone produces no observable surface cracks and no loss in tensile strength. At about 10% strain, ozone reacts rapidly with unsaturations in rubber and cracks begin to appear.¹ Under cyclic loading, when mechanical crack growth is very slow or absent, ozone cracking may be the dominant crack growth process until the cracks are large enough for flex cracking to take over. Braden and Gent² studied the propagation of a preinitiated cut in an unprotected NR (containing no antiozonant) exposed to ozone. No propagation occurred up to a certain critical load but, once this load was exceeded, the cut grew at a rate independent of the load. The characteristic tearing energy required to propagate this cut was $\sim 0.1 \text{ J/m}^2$. In contrast, in the absence of any preinitiated cut in unprotected NR, styrene/butadiene rubber (SBR), acrylonitrile/BR rubber (NBR), isobutylene/isoprene rubber (IIR), and chloroprene rubber (CR), the appearance of ozone cracking was characterized by a critical strain energy density of $\sim 10\text{--}100 \text{ kJ/m}^3$. Some of the polymers described in this work and their abbreviations are provided in Table I. The use of saturated elastomers to improve the ozone resistance of unsaturated elastomers is not new. Andrews³ studied the ozone cracking of NR blended

with an ethylene/propylene rubber (EPR). As high as 50 wt % EPR was used in his compounds. He found ozone cracks propagated across the ozone-reactive NR phase and occasionally jumped across the ozone-inert EPR particles without destroying these EPR particles. Wilchinsky and Kresge⁴ studied the ozone resistance of NR protected by 20 or 50 wt % of an ethylene/propylene/diene monomer (EPDM) rubber. They used the strain energy density estimated from the position of the boundary between the crack and uncracked regions in a loaded, tapered specimen in ozone to quantify the ozone resistance of their compounds. Doyle⁵ utilized scanning electron microscopy to study the initiation instead of the propagation of ozone cracks in NR/EPDM blend compounds. He found that ozone cracks were initiated from a layer of microvoids formed adjacent to the exposed surface and perpendicular to the applied stress, followed by the coalescence of these microvoids to open a crack in the surface.

The objective of this work is to better understand the relationships between the molecular structure [brominated isobutylene/*para*-methylstyrene (PMS) copolymer (BIMSM) structures: *para*-bromomethylstyrene (BrPMS) and PMS contents, and contour length of network chains between crosslinks (L_c)⁶] and ozone and flex cracking of BIMSM/BR/NR blend compounds. Crosslinked compounds for tire sidewall applications require minimum ozone and flex cracking. Ozone resistance is measured by the survival time of a tapered specimen under a fixed load in ozone. Different compounds are compared under the same strain energy density. The cut growth versus the

Correspondence to: M. F. Tse (mun.f.tse@exxonmobil.com).

TABLE I
Polymers and Abbreviations

Abbreviation	Description
BIMSM	Isobutylene/ <i>p</i> -bromomethylstyrene/ <i>p</i> -methylstyrene terpolymer
BR	Polybutadiene rubber
CR	Chloroprene rubber
EPDM	Ethylene/propylene/diene rubber
EPR	Ethylene/propylene rubber
EVA	Ethylene/vinyl acetate copolymer
IIR	Isobutylene/isoprene rubber
IR	Polyisoprene rubber
NBR	Acrylonitrile/butadiene rubber
NR	Natural rubber
SBR	Styrene/butadiene rubber

number of flex cycles is studied by the De Mattia flex experiment. The average molecular weight between crosslinks in the network (M_c) or the L_c of the compound is measured by solvent swelling.

EXPERIMENTAL

Materials

Several BIMSM elastomers used in this study are described in Table II. The weight and molar percentages of PMS in each polymer are provided, but the weight percentage of PMS actually refers to that of BIMSM before bromination. The molar percentage of PMS (y) was calculated from the weight percentage of PMS (x) according to the following equation:

$$y = [56x / (118 - 0.62x)] - (\text{mol \% BrPMS})$$

The structure and composition of BIMSM are shown in Figure 1. The BR used here was Budene 1207 rubber (Goodyear Tire & Rubber Company, Akron, OH), which has ~ 98% cis-1,4 content. The NR in the study was SMR 20. The carbon black fillers were N351 and N660 with specific surface areas of 73 and 35 m²/g, respectively.^{7,8}

The recipes of the BIMSM/BR/NR compounds are provided in Tables III–V. Based on a total of 100 phr

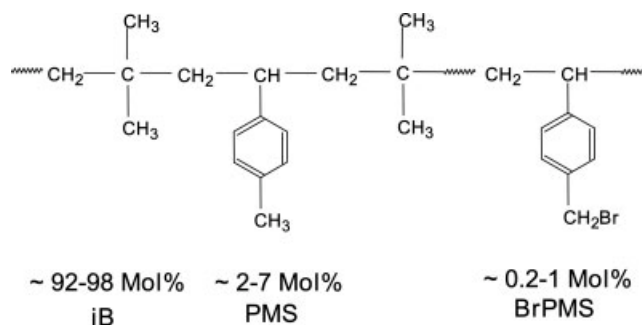


Figure 1 The BIMSM structure; iB, isobutylene.

of the combination of BIMSM, BR, and NR, each compound contains 40 phr N351, 12 phr Flexon 641, 5 phr Escorez 1102, 2 phr SP 1068, 4 phr Struktol 40MS, 0.5 phr stearic acid, 0.75 phr zinc oxide, 0.4 phr sulfur, 0.6 phr Rylex 3011, and 0.8 phr MBTS. The description and function of the compounding ingredients can be found elsewhere⁸ and are briefly provided in Table VI for reference. As shown in Table III, the BR and NR in each compound are kept at a weight ratio of about 5 : 1. We have two sets of BIMSM/BR/NR compounds with seven different BIMSM/BR/NR weight ratios. Compounds B1–B7 contain BIMSM 93-4, which has a higher BrPMS content (1.2 mol %) but a lower PMS content (7.5 wt %, Table II). In contrast, compounds B8–B14 contain BIMSM 048, which has a lower BrPMS content (0.56 mol %) but a higher PMS content (13.6 wt %). Table IV shows 12 compounds based on four different BIMSM elastomers (BIMSM 038, 048, 046, and 042) with increasing BrPMS content. All of these BIMSMs have a high PMS level of 13.6 wt %. These compounds encompass three different BIMSM/BR/NR weight ratios. Table V shows 4 other BIMSM/BR/NR compounds based on BIMSM 89-1, 96-3, 056, and 046, which all have similar molar percentages of BrPMS but various weight percentages of PMS. In addition, protected and unprotected BR/NR compounds were studied. Based on a total of 100 phr of the combination of unsaturated rubbers, the protected compound contains 50 phr BR, 50 phr NR, 50

TABLE II
Characterization of BIMSM Polymers

	BrPMS (mol %)	PMS		Mooney at 125°C	Approx. $M_n \times 10^{-3}$	Approx. $M_w \times 10^{-3}$
		wt %	mol %			
BIMSM 038	0.22	13.6	6.73	40.6	—	—
BIMSM 048	0.56	13.6	6.39	36.6	—	—
BIMSM 046	0.77	13.6	6.18	41.7	—	—
BIMSM 89-1	0.75	5.0	1.69	35	200	470
BIMSM 96-3	0.75	7.5	2.96	40	170	440
BIMSM 056	0.78	9.5	3.97	35	—	—
BIMSM 042	0.97	13.6	5.98	37.9	—	—
BIMSM 93-4	1.2	7.5	2.51	38	170	420

TABLE III
BIMSM/BR/NR Compounds

	B1	B2	B3	B4	B5	B6	B7	B8	B9	B10	B11	B12	B13	B14
BIMSM 93-4	35	40	45	50	55	60	65	—	—	—	—	—	—	—
BIMSM 048	—	—	—	—	—	—	—	35	40	45	50	55	60	65
BR	54	50	46	42	37	33	29	54	50	46	42	37	33	29
NR	11	10	9	8	8	7	6	11	10	9	8	8	7	6
t_{90} at 180°C (min)	4.2	4.2	3.9	4.0	4.1	4.2	4.6	4.2	4.1	4.1	3.8	3.8	4.0	4.0
$\sigma_{135\%}$ (MPa)	2.0	2.3	2.4	2.7	3.2	3.5	4.1	1.3	1.3	1.4	1.5	1.5	1.7	1.8
σ_b (MPa)	12	13	12	12	12	12	11	14	15	16	15	14	14	14
ϵ_b (%)	530	510	460	420	380	380	310	760	810	810	760	730	720	700

phr N660, 10 phr Flexon 641, 5 phr Escorez 1102, 3 phr 6PPD, 3 phr Sunolite 240, 2 phr stearic acid, 3 phr ZnO, 1 phr TMQ, 2 phr sulfur, and 1 phr TBBS. The unprotected compound is as above without any 6PPD, Sunolite 240, and TMQ.

Procedures

Mixing of the compounds was performed in a Banbury mixer (started at $\sim 65^\circ\text{C}$, mixed for ~ 5 min, and discharged at $\sim 150^\circ\text{C}$), followed by sheeting on a two-roll mill for the addition of curing agents. The number of minutes to 90% of maximum torque (t_{90}) values of the compounds were measured at 180°C with a moving die rheometer. The mixes in Table III were molded at 180°C for 15 min, which was longer than all the t_{90} values of the compounds, for the tensile, ozone cracking, and De Mattia samples. The mixes in Tables IV and V were molded at 180°C for 6 min for the tensile and ozone cracking samples but 10 min for the De Mattia samples. The BR/NR compounds were molded at 180°C for 10 min. The curing times used were again longer than the t_{90} values of all these compounds. Molded pads (~ 2 -mm thickness) were die cut into appropriate dimensions for viscoelastic, stress-strain, solvent swelling, and ozone cracking measurements, which are described later.

Isochronal dynamic mechanical thermal analysis (DMTA) experiments at 1 Hz were performed with a dynamic mechanical thermal analyzer (DMTA Mark II) operating in bending mode (dual cantilever,

flat face/small frame geometry) with a strain of $\sim 0.25\%$. The sample was a $35 \times 13 \times 2$ mm³ rectangle.

Molded samples were also die cut into microdumbbell specimens having a base of about 1×1 cm² and a center, narrow strip section of about 0.6×0.2 cm². Tensile stress-strain measurements were performed at a crosshead speed of 50.8 cm/min at room temperature in a tensile testing machine. These experiments were also performed at a crosshead speed of 0.64 cm/min and a temperature of 40°C . The latter conditions were used as an attempt to simulate closely what happens to the loaded elastomer samples in the ozone chamber. For both test conditions, the stress was calculated based on the undeformed cross-sectional area of the tensile specimen and the strain measurements were based on clamp separation. The strain energy density (U) at a given strain was determined by integrating the area under the stress-strain curve.

The static ozone resistance of the blend compounds was studied using the tapered specimens shown in Figure 2. These tapered specimens had the same dimensions as described by Wilchinsky and Kresge.⁴ Different weights were hung on the sample to produce different maximum strains at the narrowest section of the sample. The number of days the sample failed (broken at the narrowest section) in the ozone chamber with 0.5 ppm ozone and 40°C temperature was observed. As shown in Figure 2, the tapered specimen had an original gauge length (L_0). A weight was hung on it to elongate the sample to a certain length (L). Therefore, the average strain in the sample was

TABLE IV
BIMSM/BR/NR Compounds

	A1	A2	A3	A4	A5	A6	A7	A8	A9	A10	A11	A12
BIMSM 038	40	45	50	—	—	—	—	—	—	—	—	—
BIMSM 048	—	—	—	40	45	50	—	—	—	—	—	—
BIMSM 046	—	—	—	—	—	—	40	45	50	—	—	—
BIMSM 042	—	—	—	—	—	—	—	—	—	40	45	50
BR	50	46	42	50	46	42	50	46	42	50	46	42
NR	10	9	8	10	9	8	10	9	8	10	9	8
t_{90} at 180°C (min)	3.6	3.6	3.5	3.7	3.8	3.7	3.7	3.6	3.6	3.3	3.3	3.5
$\sigma_{135\%}$ (MPa)	1.2	1.0	1.2	1.5	1.3	1.3	1.3	1.6	1.5	1.6	1.7	1.6
σ_b (MPa)	11	12	12	15	15	15	14	12	14	12	15	13
ϵ_b (%)	870	890	890	760	820	830	740	670	730	610	720	670

TABLE V
BIMSM/BR/NR Compounds at 50 phr BIMSM

	C1	C2	C3	C4
BIMSM 89-1	50	—	—	—
BIMSM 96-3	—	50	—	—
BIMSM 056	—	—	50	—
BIMSM 046	—	—	—	50
BR	42	42	42	42
NR	8	8	8	8
t_{90} at 180°C (min)	4.0	4.0	4.0	3.9
$\sigma_{100\%}$ (MPa)	1.2	1.2	1.3	1.1
σ_b (MPa)	13	13	12	14
ϵ_b (%)	670	660	630	700

$(L - L_0)/L_0$. However, the narrowest section of the sample experienced maximum strain because of the tapering width. For example, if the average strain in the sample was 100%, the maximum strain at the narrowest section was then as high as 250% (Fig. 3). The dynamic ozone resistance of the BIMSM/BR/NR compounds was studied by repeatedly elongating a dumbbell specimen to a strain amplitude of 60% at a frequency of 30 cycles/min until complete breakage occurred in an ozone chamber at 0.5 ppm ozone and 40°C. The failure time was recorded.

Transmission electron microscopy (TEM) samples were prepared by cryomicrotoming thin sections of the molded compounds, followed by staining with osmium tetroxide. Measurements were carried out using a Philips EM 300 TEM apparatus with an accelerating voltage of 100 kV.

De Mattia flex experiments are detailed elsewhere.⁶ The test specimen was first pierced with an initial cut length ($2c_0$) of 2 mm. The cut length ($2c$) was measured at regular intervals up to ~ 2200 kilocycles. Values of the net cut length [$2(c - c_0)$] were used to rate

different elastomer compounds. Solvent swelling measurements are provided elsewhere.^{6,9}

RESULTS AND DISCUSSION

Ozone cracking behavior

Different BIMSM parts per hundred parts of rubber and BrPMS molar percentages produce different tensile properties in the BIMSM/BR/NR compounds in Tables III and IV. The modulus at 135% strain ($\sigma_{135\%}$), the tensile strength (σ_b), and the strain at break (ϵ_b) measured at room temperature and a pulling speed of 50.8 cm/min are provided in the tables. It is not informative to compare the ozone resistance of these compounds using a constant average strain applied to the sample because the strain energy density or deformation energy (U) in a higher modulus compound is higher than that in a lower modulus compound. It is more appropriate to compare the resistance at a given U (measured here at 40°C and a pulling speed of 0.64 cm/min to simulate closely what the loaded compounds experience in the ozone chamber).

Effects of BIMSM content on ozone cracking

The results for BIMSM 93-4 based compounds B1, B2, and B3 in Table III and the protected and unprotected BR/NR compounds are shown in Figure 4, which plots the days to fail in ozone as a function of the U applied to the compounds. The vertically upward direction of this figure represents better ozone resistance because the sample can survive longer in the ozone chamber. For a given compound, a higher U value will cause the sample to fail in a shorter time. At 35 phr BIMSM, blend compound B1 has ozone re-

TABLE VI
Additives and Abbreviations

Abbreviations	Description	Function
6PPD	<i>N</i> -1, 3-Dimethylbutyl- <i>N'</i> -phenyl- <i>p</i> -phenylenediamine	Antiozonant
Escorez 1102	Aliphatic petroleum resin	Tackifier
Flexon 641	Naphthenic oil	Plasticizer, softener
MBTS	Benzothiazyl disulfide	Organic accelerator
N351	Carbon black	Reinforcing filler
N660	Carbon black	Reinforcing filler
Rylex 3011	Flakes loaded with sulfur	Crosslinking agent
SP 1068	Alkyl phenol formaldehyde resin	Tackifier
—	Stearic acid	Accelerator activator
Struktol 40MS	Mixture of aliphatic/naphthenic/aromatic resins	Homogenizing/wetting agent for blending rubbers and fillers
—	Sulfur	Crosslinking agent
Sunolite 240	Blends of petroleum waxes	Nonstaining antiozonant
TBBS	80% <i>N</i> - <i>t</i> -Butyl-2-benzothiazyl sulfenamide in EPDM/EVA binder	Accelerator
TMQ	Polymerized 2,2,4-trimethyl-1,2-dihydroquinoline	Antioxidant
ZnO	Zinc oxide	Accelerator activator
Zn(OT) ₂	Zinc di-2-ethylhexanoate	Crosslinking agent

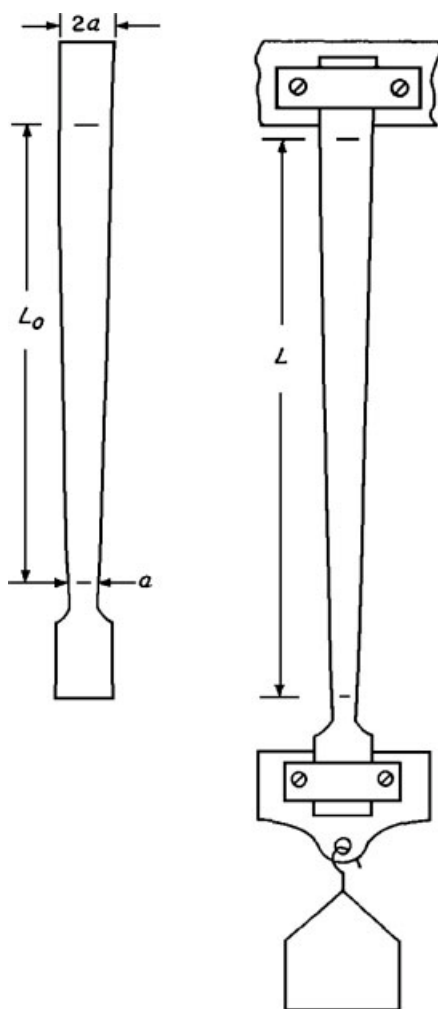
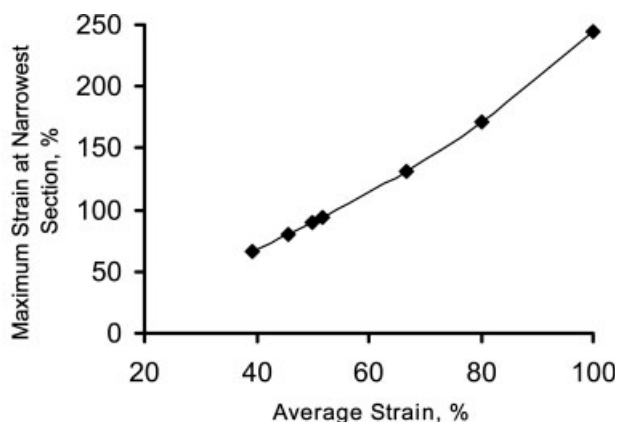


Figure 2 A description of the static ozone resistance measurement.

sistance similar to the unprotected BR/NR compound (Fig. 4). At 5 phr higher BIMSM, blend compound B2 has higher ozone resistance than the unprotected BR/



Japs/Ozone/MT1171

Figure 3 The loaded, tapered sample has different strains along its length; the narrowest section has the maximum strain.

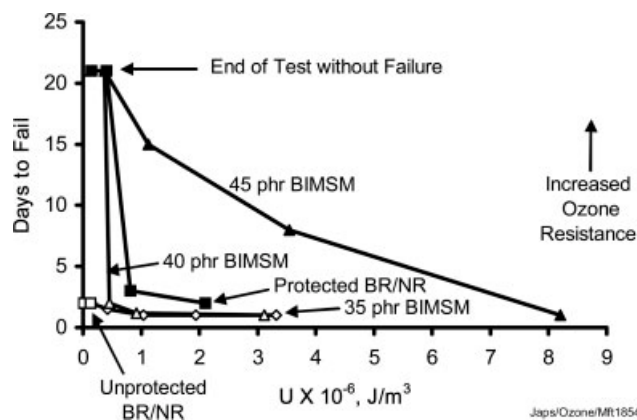


Figure 4 A higher parts per hundred parts of rubber BIMSM improves ozone resistance for BIMSM 93-4/BR/NR blend compounds; BIMSM 93-4 has 1.2 mol % BrPMS and 7.5 wt % PMS. (◇) Blend compound B1, (△) blend compound B2, (▲) blend compound B3, (□) unprotected BR/NR, and (■) protected BR/NR.

NR, but it is still inferior to the protected BR/NR (Fig. 4). At another 5 phr higher BIMSM, blend compound B3 has higher ozone resistance than the protected BR/NR (Fig. 4).

Without reproducing all the data here, we have found that all the compounds containing ≥ 50 phr BIMSM in Tables III and IV have good ozone resistance. They survive many days without breaking in the ozone chamber at some high values of U . The only exception is the compound containing 50 phr of 0.22 mol % BrPMS BIMSM (A3), which performs marginally lower than the protected BR/NR compound. As described later, at lower parts per hundred parts of rubber (40 and 45) BIMSM, the “higher BrPMS BIMSM/BR/NR” compounds perform better than or equal to the protected BR/NR compound. Therefore, lower levels of BrPMS will not improve the ozone resistance and performance of this kind requires the addition of a higher amount of BIMSM. Although these 0.22 mol % BrPMS BIMSM/BR/NR compounds have excellent cut growth resistance (described later), their ozone resistance is not acceptable.

As described previously, without any preinitiated cut in unprotected NR, SBR, NBR, IIR, and CR, the critical U value for the onset of ozone cracking is $\sim 10\text{--}100$ kJ/m³. According to Figure 4, we operated our ozone experiments at a much higher U level in order to fail our BIMSM/BR/NR blend compounds without any antiozonants. Therefore, BIMSM functions as the ozone-inert phase of the blend and it is not surprising to observe that a higher BIMSM content improves the ozone resistance of each set of BIMSM/BR/NR compounds based on a given BIMSM (Tables III, IV).

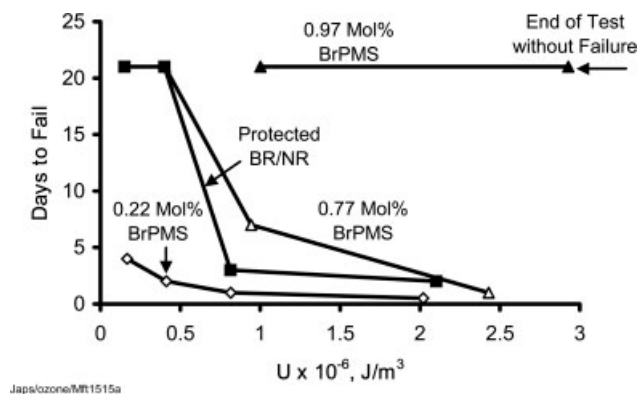


Figure 5 A higher mole percentage of BrPMS in BIMSM improves the ozone resistance of BIMSM/BR/NR blend compounds containing 45 phr BIMSM. The BIMSMs have identical PMS content (13.6 wt %) but different BrPMS contents.

Effects of BrPMS content in BIMSM on ozone cracking

Figure 5 shows a plot similar to Figure 4 except it compares the ozone resistance of blend compounds based on 45 phr BIMSM. Blend compounds A2, A8, and A11 in Table IV contain BIMSM 038, 046, and 042, which have 0.22, 0.77, and 0.97 mol % BrPMS, respectively. The PMS content of each BIMSM is at a constant level of 13.6 wt % (Table II). Clearly, the higher BrPMS BIMSM/BR/NR compounds perform better than the lower BrPMS BIMSM/BR/NR compounds. Compound A11 survives beyond 21 days without breaking in the ozone chamber, even when the U value is as high as $3 \times 10^6 \text{ J/m}^3$. This behavior is also observed for compounds A1, A7, and A10, which contain 40 phr BIMSM 038, 046, and 042, respectively. The higher BrPMS BIMSM/BR/NR compounds are more ozone resistant than the lower BrPMS BIMSM/BR/NR compounds. Of course, A10 is not as good as A11 because of lower BIMSM content. The former compound fails in 1 day in the ozone chamber when the U value is about $3 \times 10^6 \text{ J/m}^3$.

A possible explanation for the higher ozone resistance of the higher BrPMS BIMSM/BR/NR compound is its higher crosslink density (described later). Overall, higher crosslink density is also reflected by a higher $\sigma_{135\%}$ and a lower ϵ_b of the compound (Tables III, IV). A higher crosslink density could reduce chain mobility, lowering ozone diffusing and cracking rates, and consequently producing a higher protection to ozone attack.

Effects of PMS content in BIMSM on ozone cracking

The ozone cracking results of some compounds in Table III are provided in Figure 6. These results again show that a higher BIMSM content improves the

ozone resistance of each set of BIMSM/BR/NR compounds based on a given BIMSM. The amount of BIMSM 93-4 in B1, B3, B5, and B7 is increased from 35 to 65 phr, which is also the same amount for BIMSM 048 in B8, B10, B12, and B14. The filled and open symbols in this figure represent blend compounds containing BIMSM 93-4 and 048, respectively. In addition, at first sight, Figure 6 seems to suggest that the lower BrPMS BIMSM/BR/NR compounds perform better than the higher BrPMS BIMSM/BR/NR compounds for a given BIMSM content (B1 and B8 at 35 phr BIMSM, B3 and B10 at 45 phr BIMSM, B5 and B12 at 55 phr BIMSM, and B7 and B14 at 65 phr BIMSM). However, as shown in Table II, the 0.56 and 1.2 mol % BrPMS BIMSMs have 13.6 and 7.5 wt % PMS, respectively. We speculate that the better ozone resistance of the 0.56 mol % BrPMS BIMSM/BR/NR compounds compared to the 1.2 mol % BrPMS BIMSM/BR/NR compounds is not due solely to the effects of BrPMS; rather, it is due to the effect of PMS. More evidence is presented in Figure 7, which compares the dynamic ozone testing data of four BIMSM/BR/NR compounds based on 50 phr BIMSMs at a similar mole percentage of BrPMS but different weight percentages of PMS (Table V). The higher PMS BIMSM/BR/NR compound has better dynamic ozone resistance. Under the same dynamic ozone test conditions, the protected BR/NR fails in 2 days. Theoretically, a high PMS level should result in lower interfacial tension between the BIMSM and BR/NR phases, producing a morphological state of a finer structure. The result is better protection to the corrosive attack of ozone. The higher PMS level may also influence carbon black distribution, resulting in a more favorable phase volume relationship at a constant parts per hundred parts of rubber value.¹⁰

The degree of compatibility of BIMSM and BR/NR phases in the BIMSM/BR/NR compounds was

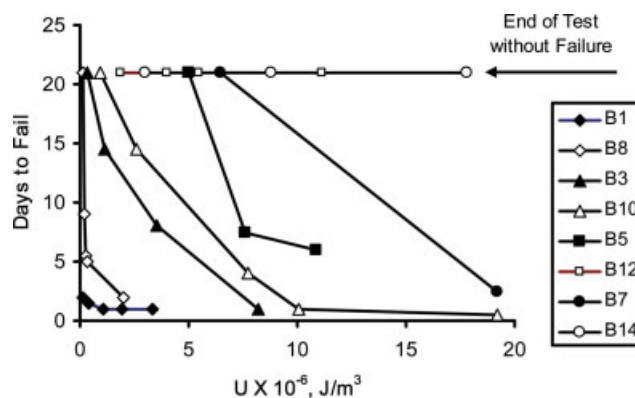
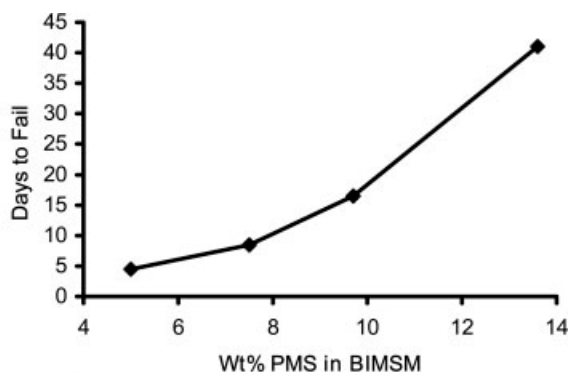


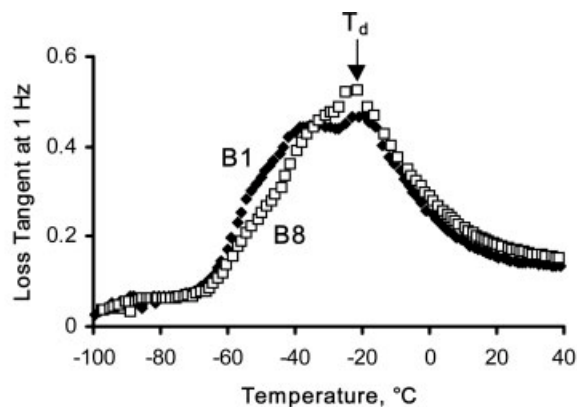
Figure 6 Overall, a higher weight percentage of PMS in BIMSM improves the ozone resistance of BIMSM/BR/NR blend compounds. [Color figure can be viewed in the online issue, which is available at www.interscience.wiley.com.]



Japs/Ozone/Mfr1546

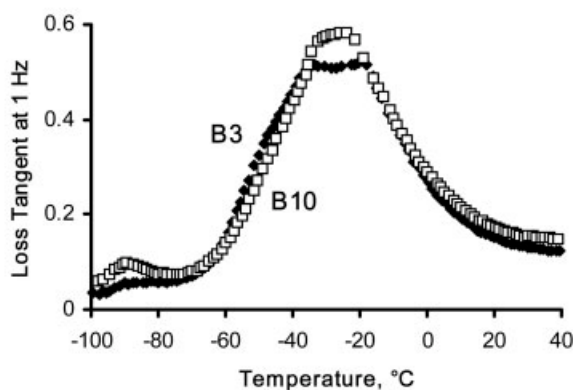
Figure 7 The dynamic ozone resistance of BIMSM/BR/NR blends confirms the importance of high PMS in BIMSM.

studied by DMTA measurements. These provided indirect evidence for the above hypothesis that a high PMS level in BIMSM will improve the compatibility between the BIMSM and BR/NR phases. The DMTA results of the same set of compounds in Figure 6 are shown in Figure 8, which illustrates the temperature dependence of the loss tangent measured at 1 Hz for compounds at 35, 45, 55, and 65 phr BIMSM. The peaks in these curves are used to locate the transition temperatures of the BIMSM/BR/NR compounds. Curves with filled symbols are loss tangent curves of BIMSM/BR/NR compounds based on BIMSM 93-4 (1.2 mol % BrPMS, 7.5 wt % PMS), whereas curves with open symbols are loss tangent curves of BIMSM/BR/NR compounds based on BIMSM 048 (0.56 mol % BrPMS, 13.6 wt % PMS).



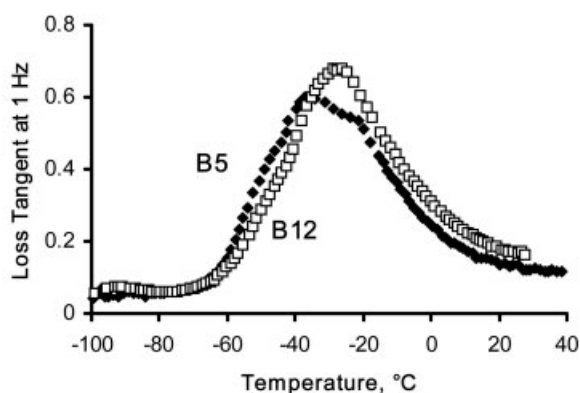
Japs/Ozone/Mfr1226

(a)



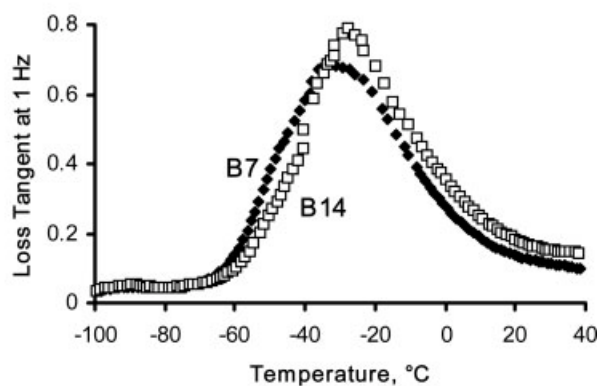
Japs/Ozone/Mfr1227

(b)



Japs/Ozone/Mfr1229

(c)



Japs/Ozone/Mfr1225

(d)

Figure 8 Loss tangent curves of (a) B1 and B8, each containing 35 phr BIMSM; (b) B3 and B10, each containing 45 phr BIMSM; (c) B5 and B12, each containing 55 phr BIMSM; and (d) B7 and B14, each containing 65 phr BIMSM. Curves with filled symbols are loss tangent curves of BIMSM/BR/NR compounds based on BIMSM 93-4 (1.2 mol % BrPMS, 7.5 wt % PMS); curves with open symbols are loss tangent curves of BIMSM/BR/NR compounds based on BIMSM 048 (0.56 mol % BrPMS, 13.6 wt % PMS).

The basic concept to discern the difference in compatibility is based on the fact that BIMSM has an additional damping peak temperature (T_d) above its glass-transition temperature (T_g), even though BIMSM and NR have very similar T_g values ($T_g < T_d$).^{11,12} Because the BR phase has a T_g at approximately -90°C , which is well separated from the NR T_g and BIMSM T_d , we can deduce the degree of compatibility of the BIMSM and BR/NR phases by examining how the T_g of NR and the T_d of BIMSM are shifted in a blended compound. A smaller difference in the NR T_g and BIMSM T_d or a narrower composite loss tangent peak suggests better compatibility. Based on this criterion, the high-PMS BIMSM/BR/NR compound appears to have better compatibility between BIMSM and BR/NR than the low-PMS BIMSM/BR/NR compound for BIMSM contents ranging from 35 to 65 phr.

Morphology

To further understand the effects of the parts per hundred parts of rubber BIMSM and PMS content on the blend phase morphology and ozone resistance, we studied the morphology of the blend compounds by TEM and image analysis. Figure 9(a) is a TEM picture of the blend compound (B3 in Table III) containing 45 phr BIMSM 93-4. The white area is the BIMSM phase, the gray (light blue online) area is the diene polymer (BR/NR) phase, the black area is the carbon

black filler, and the white bar at the bottom is a scale of $1\ \mu\text{m}$. By image analysis, we can outline the BIMSM phase with gray (red online) lines and then fill in this phase with gray [red online, Fig. 9(b)]. We can also darken the originally gray (blue online) color of the diene polymer phase to distinguish it from the BIMSM phase. The result is a picture clearly showing the percentage of area covered by the filled BIMSM phase (gray, red online) and the percentage of area covered by the filled diene polymer phase [black, dark blue online, Fig. 9(c)]. Therefore, a picture like this can help us quantify the continuity of either the BIMSM or the diene polymer phase.

By applying this method to the blend compound (B2, Table III) containing 40 phr BIMSM 93-4, we obtained the picture shown in Figure 10(a), where the gray (red online) area is the filled BIMSM phase, the black (dark blue online) area is the filled diene polymer phase, and the gray (red online) bar at the bottom is a scale of $1\ \mu\text{m}$. We then divide this into 16 cells and notice that the percentage of area covered by BIMSM varies in each cell. For example, as marked in Figure 10(a), the BIMSM area coverage in one cell is 61%, which should have good ozone resistance, but that in the other cell is only 15%, which should have poor ozone resistance. Based on this analysis, we constructed the histogram in Figure 10(b). There are 2 cells with 9–18% BIMSM area coverage, 5 cells with 18–28% BIMSM area coverage, 2 cells with 28–38% BIMSM area coverage (equivalent

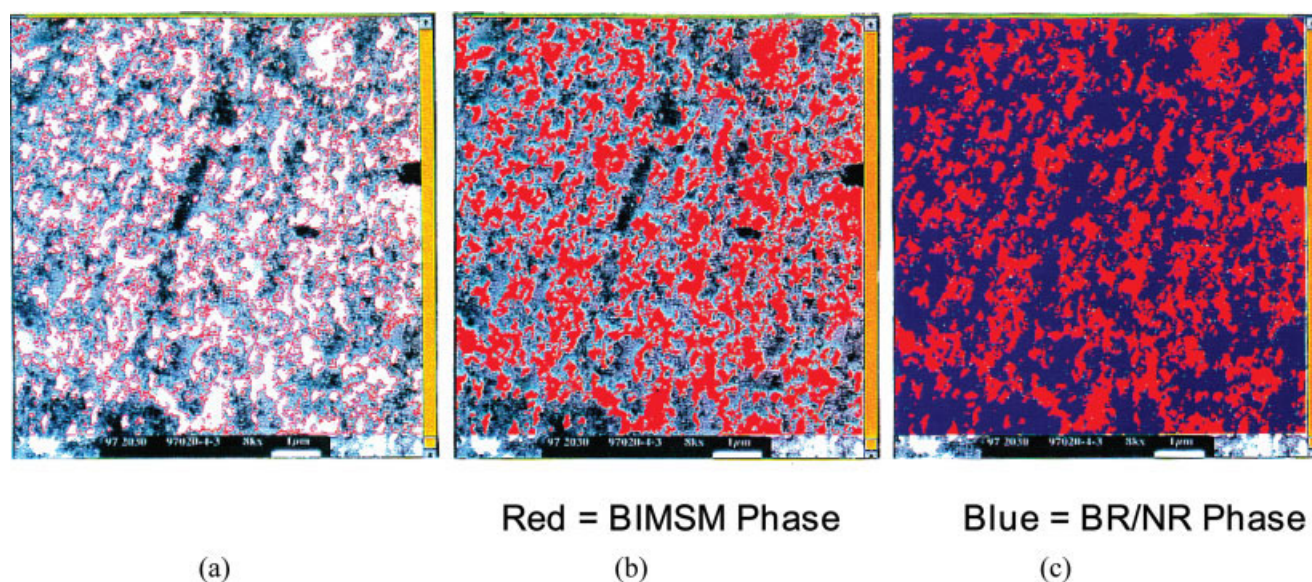


Figure 9 TEM image analysis can quantify the phase continuity for the BIMSM/BR/NR blend containing 45 phr BIMSM 93-4. (a) White area, BIMSM phase; gray area (light blue online), diene polymer (BR/NR) phase; black area, carbon black filler; scale bar = $1\ \mu\text{m}$. (b) By image analysis we outline the BIMSM phase with gray (red online) lines and then fill in this phase with gray (red online). We also darken the originally gray (blue online) color of the diene polymer phase to distinguish it from the BIMSM phase. (c) The result is a picture clearly showing the percentage of area covered by the filled BIMSM phase (gray, red online) and the percentage of area covered by the filled diene polymer phase (black, dark blue online). [Color figure can be viewed in the online issue, which is available at www.interscience.wiley.com.]

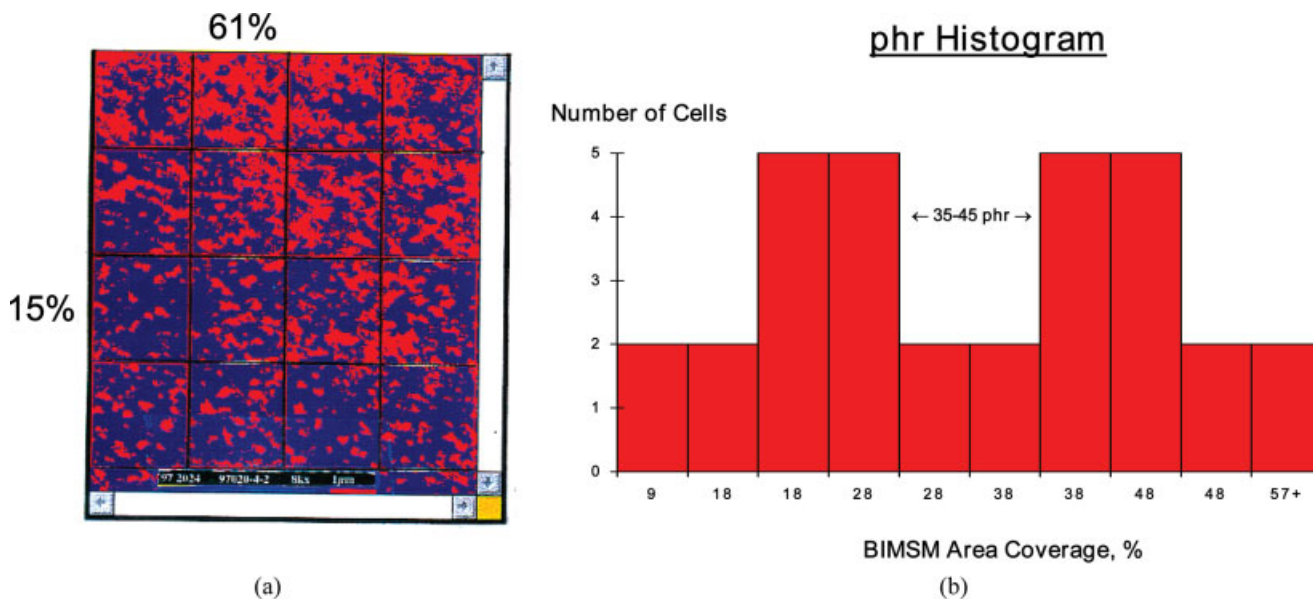


Figure 10 Forty parts per hundred parts of rubber BIMSM is actually a distribution of parts per hundred parts of rubber in microscopic scale; BIMSM 93-4 has 1.2 mol % BrPMS and 7.5 wt % PMS. (a) The gray area (red online) is the filled BIMSM phase, and the black area (dark blue online) is the filled diene polymer phase; scale bar = 1 μ m. (b) A histogram based on the analysis. [Color figure can be viewed in the online issue, which is available at www.interscience.wiley.com.]

to 35–45 phr BIMSM), 5 cells with 38–48% BIMSM area coverage, and 2 cells with 48–57+% BIMSM area coverage. The number of cells still adds up to a total of 16. What this histogram suggests is that 40 phr BIMSM is actually a bimodal distribution of parts per hundred parts of rubber on the microscopic scale. In other words, 40 phr BIMSM 93-4 in the blend compound may not be perfect for ozone protection because of this blend phase morphology,

which is possibly the result of poor mixing between BIMSM 93-4 and BR/NR. Conversely, 40 phr BIMSM 048 in the blend compound (B9, Table III) shows a more uniform parts per hundred parts of rubber distribution (Fig. 11). Therefore, a higher amount of PMS in BIMSM improves its mixing with BR/NR, producing higher ozone resistance for the blend compound. This is consistent with our ozone cracking results illustrated in Figures 6 and 7. Figure 12

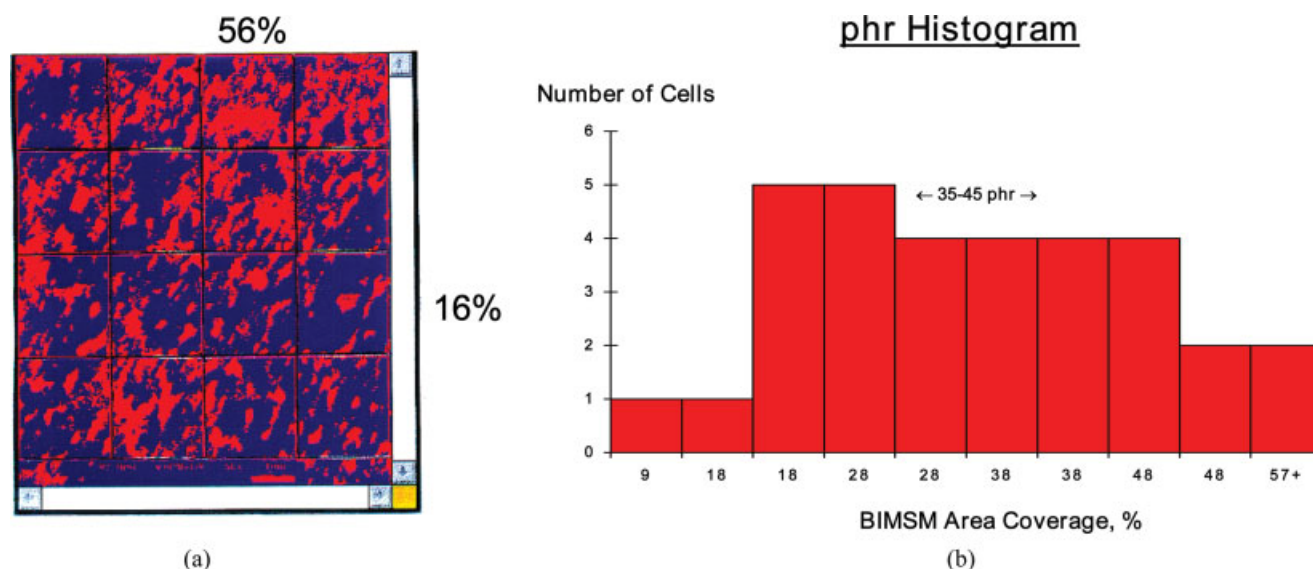


Figure 11 Forty parts per hundred parts of rubber BIMSM is actually a distribution of parts per hundred parts of rubber in microscopic scale; BIMSM 048 has 0.56 mol % BrPMS and 13.6 wt % PMS. [Color figure can be viewed in the online issue, which is available at www.interscience.wiley.com.]

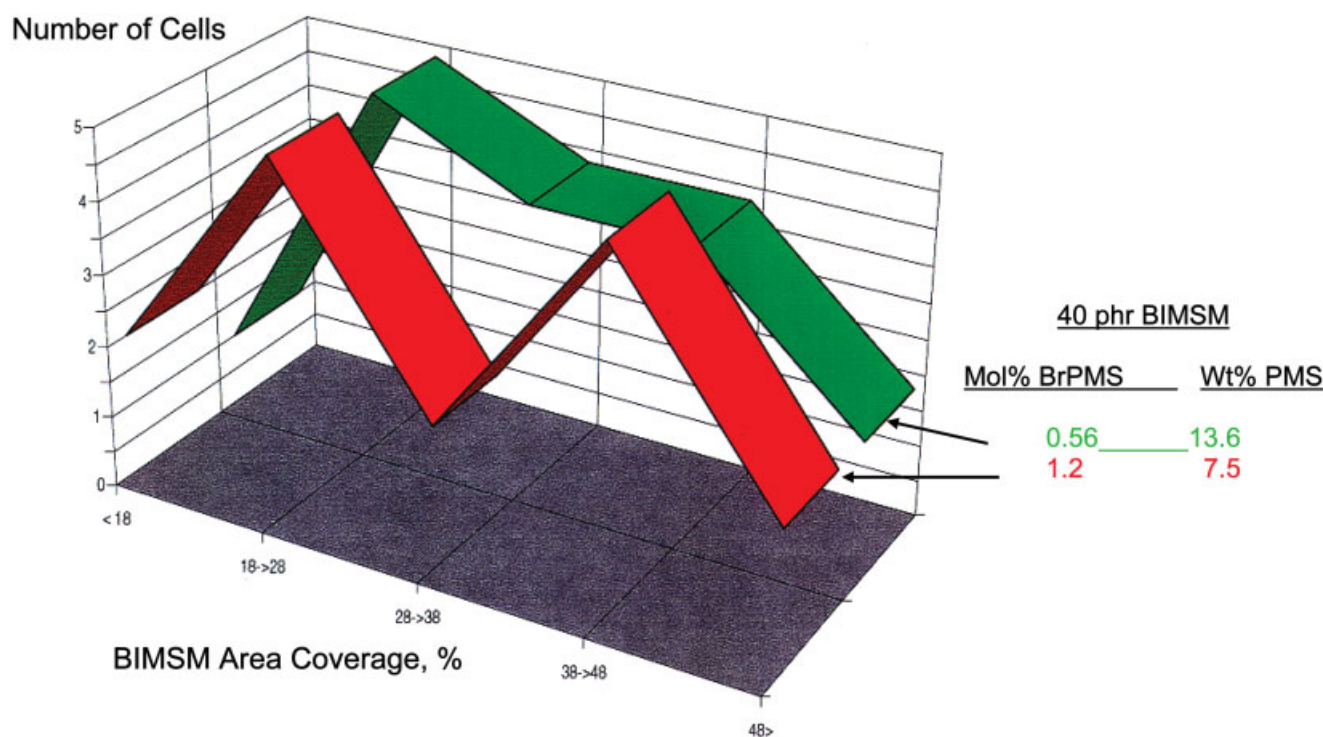


Figure 12 BIMSM with a higher PMS distributes more uniformly in the BIMSM/BR/NR blend. [Color figure can be viewed in the online issue, which is available at www.interscience.wiley.com.]

summarizes the results of the parts per hundred parts of rubber histograms in Figures 10 and 11 for 40 phr BIMSM 93-4 and 048 in the blend compounds. Therefore, BIMSM with a higher amount of PMS distributes more uniformly in the blend compound, enhancing the ozone resistance.

Figure 13 compares the blend phase morphology of BIMSM/BR/NR blend compounds at 40, 45, and 50 phr BIMSM based on TEM and image analysis. The upper and lower rows are blend compounds based on BIMSM 93-4 and 048, respectively. Some of these pictures were shown in Figures 9–11. It appears that a cocontinuous phase morphology requires *at least* 45–50 phr BIMSM. This is consistent with our ozone cracking results that a higher BIMSM content improves the ozone resistance of the blend compounds. In addition, BIMSM 048 with a higher weight percentage of PMS improves the phase morphology of the blend compound as evidenced by the micrographs (45 and 50 phr BIMSM) in the lower row of Figure 13.

De Mattia flex cracking behavior

A previous study demonstrated that a lower molar percentage of BrPMS in a neat BIMSM compound improves the De Mattia cut growth resistance because the L_c exceeds a certain critical value.⁶ This behavior appears to be true for BIMSM blended with BR/NR. Figure 14 shows the growth of the De Mattia preinitiated

cut as a function of flex cycles for BIMSM/BR/NR compounds at 50 phr BIMSM (compounds A3, A6, A9, and A12, Table IV). The lower BrPMS BIMSM/BR/NR compound has a higher cut growth resistance. This is also clearly reflected in Figures 15 and 16, which show the growth of the preinitiated cut as a function of flex cycles for compounds B1–B7 and B8–B14 (Table III), respectively. At a given parts per hundred parts of rubber BIMSM, the 0.56 mol % BrPMS BIMSM/BR/NR compound has higher cut growth resistance than the 1.2 mol % BrPMS BIMSM/BR/NR compound (note that Figs. 15 and 16 have different vertical scales). Overall, the cut growth resistance is higher at a lower parts per hundred parts of rubber BIMSM for BIMSM in the range of 35–65 phr. Conversely, the PMS content in BIMSM seems not to affect the cut growth significantly as described in Figure 17, which shows the results of four compounds at 50 phr BIMSM (Table V).

In our previous study of single polymer and compatible blend compounds,⁶ we also found that, above a critical L_c of about 60–70 nm, the cut growth of the compound is slow and stable. By contrast, the cut growth is fast or catastrophic if the L_c is below 60–70 nm. To test whether this critical L_c model is true for phase-separated BIMSM/BR/NR compounds, we plot the De Mattia cut length of all the compounds in Tables III and IV at three different flex cycles (4.5, 400, and 2200 kilocycles) as a function of the average L_c in

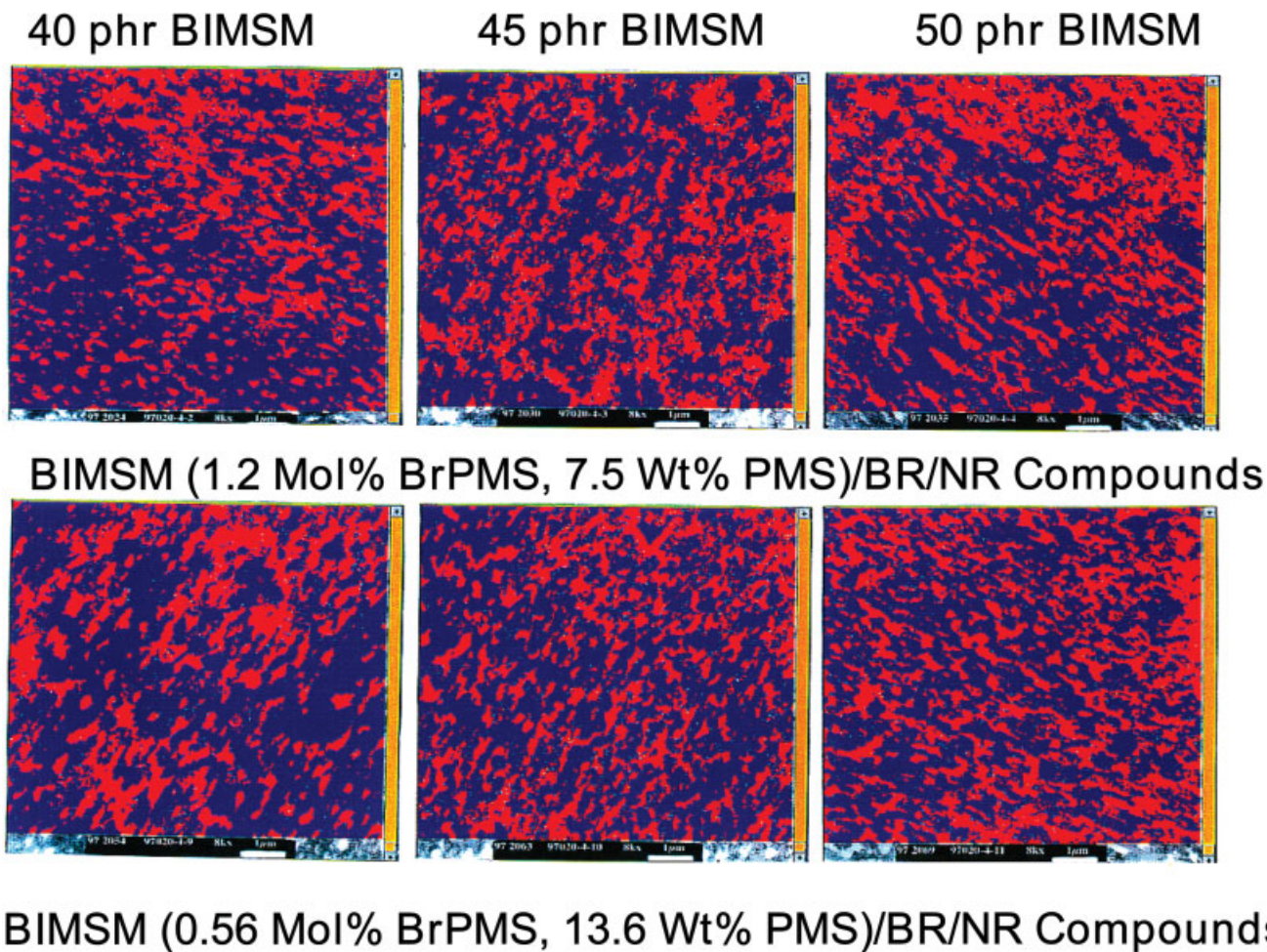


Figure 13 A cocontinuous morphology requires 45–50 phr BIMSM in the blend. [Color figure can be viewed in the online issue, which is available at www.interscience.wiley.com.]

Figure 18(a–c). The L_c value, which is determined from solvent swelling, is the average value in the BIMSM and the BR/NR phase. The high-BrPMS

BIMSM has 0.77, 0.97, or 1.2 mol % BrPMS whereas the low-BrPMS BIMSM has 0.22 or 0.56 mol % BrPMS. At a low flex cycle (4.5 kilocycles), the preinitiated cuts of four of the high-BrPMS BIMSM/BR/NR compounds propagate beyond 5 mm. Those of the other

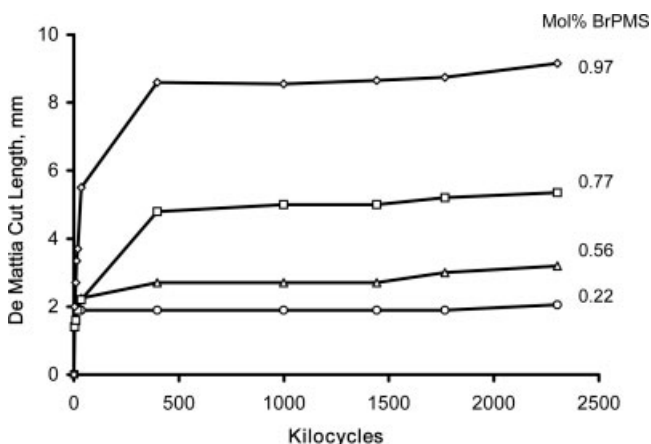


Figure 14 A lower BrPMS BIMSM improves the cut growth resistance of BIMSM/BR/NR compounds at 50 phr BIMSM (Table IV).

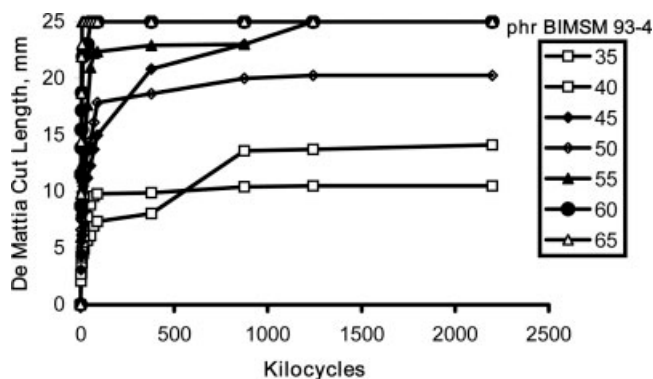


Figure 15 The dependence of the cut growth behavior of BIMSM 93-4/BR/NR compounds in Table III on the parts per hundred parts of rubber BIMSM and flex cycles.

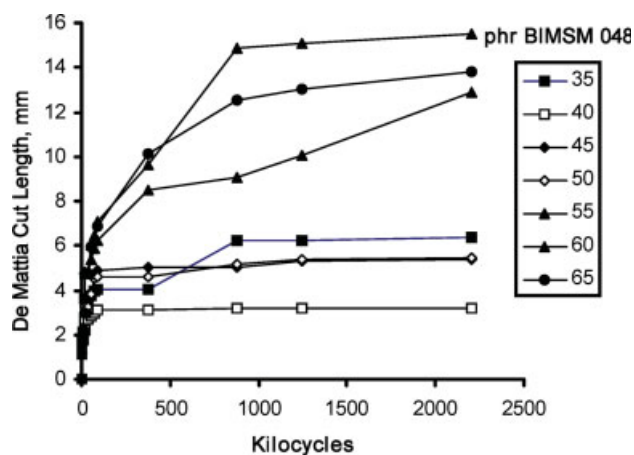


Figure 16 The dependence of the cut growth behavior of BIMSM 048/BR/NR compounds in Table III on the parts per hundred parts of rubber BIMSM and flex cycles. [Color figure can be viewed in the online issue, which is available at www.interscience.wiley.com.]

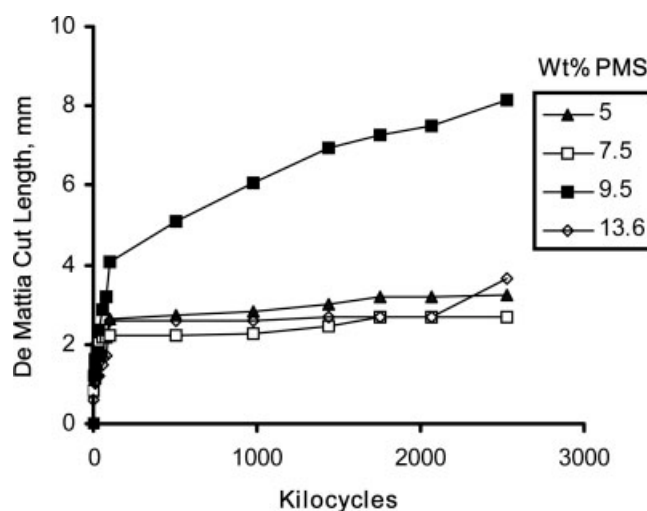
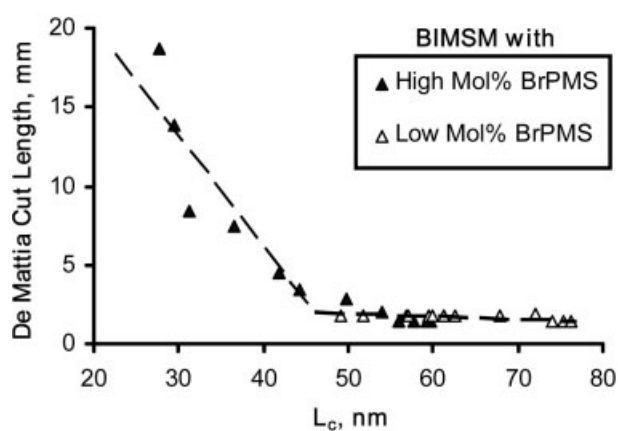
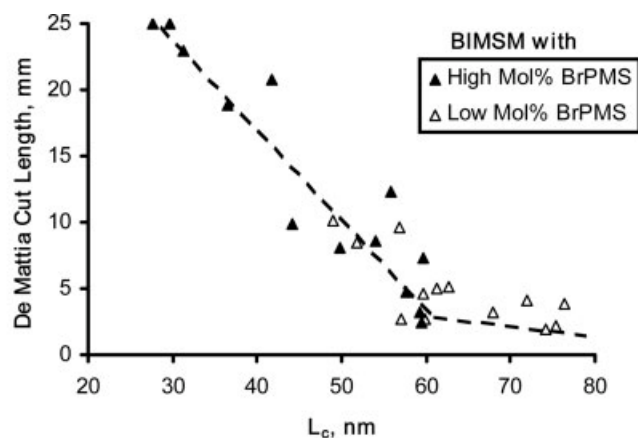


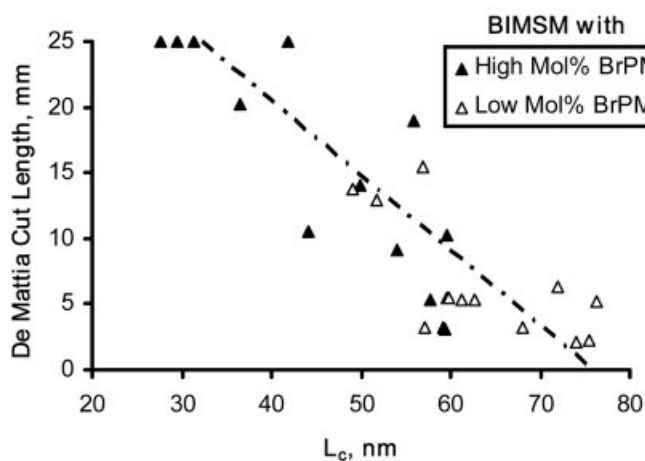
Figure 17 The dependence of the cut growth behavior of BIMSM/BR/NR blends in Table V on the weight percentage of PMS in BIMSM and flex cycles.



(a)



(b)



(c)

Figure 18 The cut growth versus the network chain length between crosslinks (L_c) for BIMSM/BR/NR blends in Tables III and IV at (a) 4.5, (b) 400, and (c) 2200 kilocycles.

compounds stay below 5 mm. The break point separating the fast and slow cut growth occurs at ~ 45 nm. Of course, the cut in each compound propagates further at a higher flex cycle (400 kilocycles). Now the break point occurs at a longer L_c (~ 60 nm), which is very close to the critical L_c of 60–70 nm for single polymer and highly compatible blend compounds.⁶ This result also suggests that a higher flex cycle requires a longer critical L_c for achieving a higher cut growth resistance. As noted, the data in Figure 18(b) for the higher flex cycle become more scattered but the reason for this is not clear. Possible explanations are variations in the cure states of the polymer phases and/or other structural variations due to mixing problems, such as the morphological difference and the difference in the blend interfacial regions when the BIMSM content is varied in these compounds. One example for the latter case is shown in Figures 10–12. The data at 2200 kilocycles are very scattered [Fig. 18(c)]. Locating a break point separating the fast and slow cut growth becomes impossible or a critical value of L_c longer than 80 nm is required to impede the cut propagation. To sum up, it appears that the cut growth L_c model developed for single polymer and compatible blend compounds can be applied with some cautions to the phase-separated BIMSM/BR/NR blend compounds. These compounds are very complex with a wide variety of cure states and morphological features containing a discrete, cocontinuous, or continuous BIMSM phase.

Figure 19 shows the values of L_c in the BIMSM and the BR/NR phases for each compound in Table III when the BIMSM content in the blend compound is varied. BIMSM 93-4/BR/NR and BIMSM 048/BR/NR blends are described. It is evident that each phase in the BIMSM 93-4/BR/NR blends is crosslinked tighter than in the BIMSM 048/BR/NR

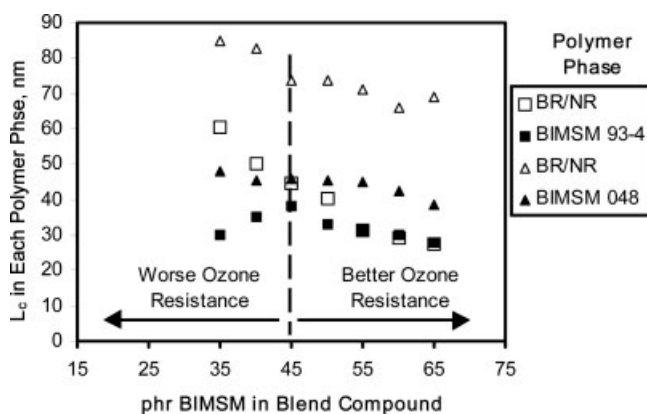


Figure 19 The value of the network chain length between crosslinks (L_c) in each polymer phase as a function of the BIMSM content for the BIMSM/BR/NR blends in Table III. BIMSM 93-4/BR/NR blends: (■) BIMSM and (□) BR/NR; BIMSM 048/BR/NR blends: (▲) BIMSM and (△) BR/NR.

blends. This explains why the former blend system has an inferior cut growth resistance (Fig. 15 vs. 16). However, the ozone resistance is improved with higher BrPMS and PMS levels in BIMSM. Therefore, we can control the crosslink density or cure state, especially in the BR/NR phase, to obtain a good balance in ozone and flex cracking. Of course, a higher BIMSM content in the blend improves the ozone resistance because BIMSM acts as the ozone-inert phase in the absence of antiozonant(s). A carefully designed BIMSM/BR/NR blend can have higher ozone resistance than a protected BR/NR blend (Fig. 4).

CONCLUSIONS

The ozone resistance and cut growth resistance of ternary blends of BIMSM/BR/NR were studied. On the one hand, ozone cracking depends on the BIMSM content and the BrPMS and PMS levels in BIMSM. A higher BIMSM content, a higher mole percentage of BrPMS, or a higher weight percentage of PMS improved the ozone resistance of these compounds. Higher amounts of BIMSM, BrPMS, and PMS increased the ozone-inert phase volume, crosslink density, and homogeneity of the blend phase morphology, respectively. On the other hand, a lower BIMSM content or a lower mole percentage of BrPMS in BIMSM improved the cut growth resistance of the BIMSM/BR/NR compound. The PMS content did not appear to produce any significant effects for the PMS contents studied. Similar to single polymer and compatible blend compounds, the cut growth resistance of the phase-separated BIMSM/BR/NR compound was also approximately controlled by the L_c . We demonstrated the existence of a critical L_c value (~ 60 nm) separating the fast and slow cut growth of these elastomer compounds when flexed to a reasonably high number of cycles (~ 400 kilocycles). Therefore, selection of the content and composition (mole percentage BrPMS, weight percentage PMS) of BIMSM for the commercial formulation of BIMSM/BR/NR blend depends on the balance of properties desired, namely, the ozone and cut growth resistance, in the in-service performance of the crosslinked compound.

I thank K. O. McElrath for his contribution to this work, J. M. Blake and M. W. Johnston for experimental assistance, and M. R. Ynostroza for TEM and image processing. Part of this article was presented at the Rubber Division Meeting, American Chemical Society, Indianapolis, Indiana, May 5–8, 1998.

References

- (a) Newton, R. G. *J Rubber Res* 1945, 14, 27; (b) Newton, R. G. *J Rubber Res* 1945, 14, 41.

2. (a) Braden, M.; Gent, A. N. *J Appl Polym Sci* 1960, 3, 90; (b) Braden, M.; Gent, A. N. *J Appl Polym Sci* 1960, 3, 100.
3. Andrews, E. H. *J Appl Polym Sci* 1966, 10, 47.
4. Wilchinsky, Z. W.; Kresge, E. N. *Rubber Chem Technol* 1974, 47, 895.
5. Doyle, M. J. Presented at the International Tire Exhibition and Conference, Akron, OH, September 10–12, 1966.
6. Tse, M. F.; McElrath, K. O.; Wang, H.-C. *Polym Eng Sci* 2002, 42, 1210.
7. Wolff, S.; Wang, M.-J.; Tan, E.-H. *Rubber Chem Technol* 1993, 66, 163.
8. Blue Book; Lippincott & Peto Inc.: Akron, OH, 1994.
9. Wang, Y. F.; Wang, H.-C. *Rubber Chem Technol* 1997, 70, 663.
10. Tse, M. F. *J Appl Polym Sci* 2006, 101, 659.
11. Tse, M. F.; Wang, H.-C.; Rogers, J. E. *Rubber World* 1997, 216, 39.
12. Ngai, K. L.; Plazek, D. J.; Rizo, A. K. *J Polym Sci Part B: Polym Phys Ed* 1997, 35, 599.